Two-gap superconductivity in $R_2Fe_3Si_5$ (R=Lu, Sc) and $Sc_5Ir_4Si_{10}$

2008 Sci. Technol. Adv. Mater. 9 044206

(http://iopscience.iop.org/1468-6996/9/4/044206)

Sci. Technol. Adv. Mater. **9** (2008) 044206 (6pp) doi:10.1088/1468-6996/9/4/044206

Two-gap superconductivity in $R_2Fe_3Si_5$ (R= Lu, Sc) and $Sc_5Ir_4Si_{10}$

Tsuyoshi Tamegai[1], Yasuyuki Nakajima[1], Tsuyoshi Nakagawa[1], Guoji Li[1] and Hisatomo Harima[2]

[1] Department of Applied Physics, The University of Tokyo, Hongo, Bunkyo-ku, Tokyo 113-8656, Japan
[2] Department of Physics, Kobe University, Kobe 657-8501, Japan

E-mail: tamegai@ap.t.u-tokyo.ac.jp

Received 22 October 2008
Accepted for publication 5 December 2008
Published 28 January 2009
Online at stacks.iop.org/STAM/9/044206

Abstract

$R_2Fe_3Si_5$ (R = Sc, Y, Lu) contains nonmagnetic iron and has a relatively high superconducting transition temperature T_c among iron-containing superconductors. An anomalous temperature dependence of specific heat $C(T)$ has been reported for polycrystalline samples down to 1 K. We have grown $R_2Fe_3Si_5$ single crystals, confirmed the anomalous $C(T)$ dependence, and found a second drop in specific heat below 1 K. In $Lu_2Fe_3Si_5$, we can reproduce $C(T)$ below T_c, assuming two distinct energy gaps $2\Delta_1/k_BT_c = 4.4$ and $2\Delta_2/k_BT_c = 1.1$, with nearly equal weights, indicating that $Lu_2Fe_3Si_5$ is a two-gap superconductor similar to MgB_2. Hall coefficient measurements and band structure calculation also support the multiband contributions to the normal-state properties. The specific heat in the $Sc_2Fe_3Si_5$ single crystals also shows the two-gap feature. $R_5Ir_4Si_{10}$ (R = Sc, rare earth) is also a superconductor where competition between superconductivity and the charge-density wave is known for rare earths but not for Sc. We have performed detailed specific heat measurements on $Sc_5Ir_4Si_{10}$ single crystals and found that $C(T)$ deviates slightly from the behavior expected for weak-coupling superconductors. $C(T)$ for these superconductors can also be reproduced well by assuming two superconducting gaps.

Keywords: two-gap superconductivity, $Lu_2Fe_3Si_5$, $Sc_2Fe_3Si_5$, $Sc_5Ir_4Si_{10}$

(Some figures in this article are in colour only in the electronic version)

1. Introduction

Several exotic silicide superconductors were discovered around 1980. $R_2Fe_3Si_5$ and $R_5Ir_4Si_{10}$ (R = Sc, Y, rare earth elements) are two typical examples of such superconductors [1, 2]. Another example is the first heavy fermion superconductor $CeCu_2Si_2$ [3]. $R_2Fe_3Si_5$ crystallizes in a tetragonal $Sc_2Fe_3Si_5$ structure and contains nonmagnetic iron with square planar and linear arrangements as shown in figure 1(a) [1]. $R_5Ir_4Si_{10}$ crystallizes in a tetragonal $Sc_5Co_4Si_{10}$ structure, and R atoms form chains in the pentagonal and hexagonal Ir–Si network along the c-axis, as shown in figure 1(b) [2]. Peculiar properties have been reported in both $R_2Fe_3Si_5$ and $R_5Ir_4Si_{10}$ in the superconducting and normal states.

$R_2Fe_3Si_5$ has one of the highest superconducting transition temperatures T_c among iron-containing superconductors ($Lu_2Fe_3Si_5$: $T_c = 6.0$ K) [1, 4], except for the recently found iron-based oxypnictides ($LaFeAsO_{1-x}F_x$: $T_c = 26$ K, $SmFeAsO_{1-x}F_x$: $T_c = 55$ K) [5, 6]. One of the most marked properties of $R_2Fe_3Si_5$ is an anomalous temperature dependence of specific heat $C(T)$ found in polycrystalline samples down to 1 K [7]. The jump of specific heat at T_c, $\Delta C/\gamma_n T_c$ (γ_n is the electronic specific heat coefficient) is reduced from the BCS (Bardeen–Cooper–Schrieffer) value of 1.43, and there are apparent residual values of specific heat coefficients in the low-temperature limit. These anomalies of $C(T)$ have been confirmed in high-quality polycrystalline samples of $Lu_2Fe_3Si_5$ [8]. However, more detailed discussion on the anomalous nature, including anisotropy, requires

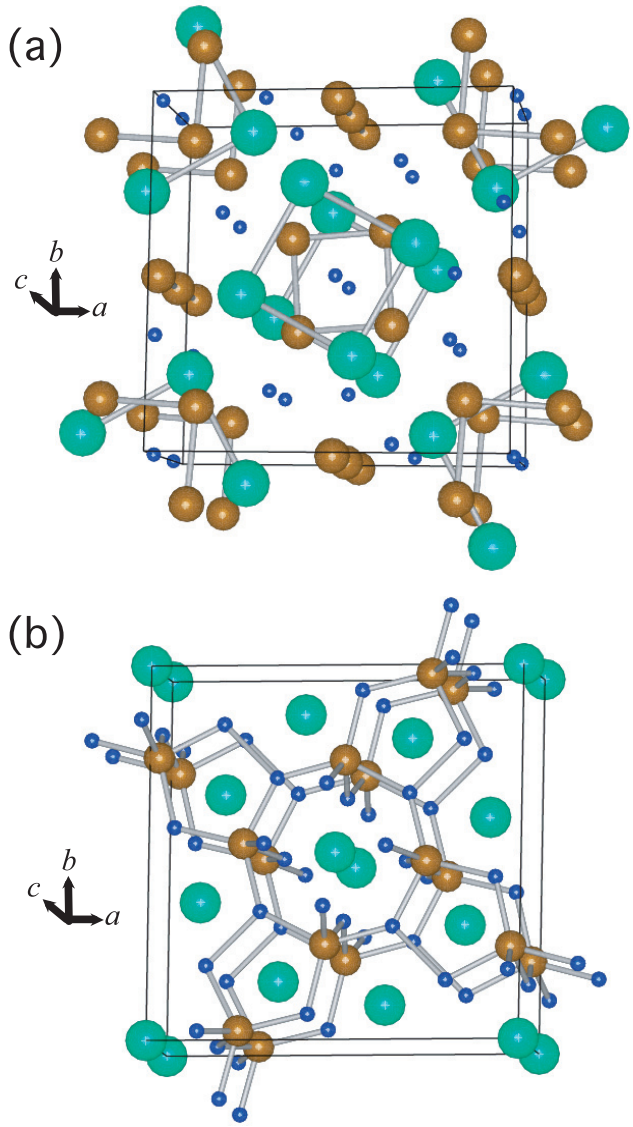

Figure 1. Crystal structures of (a) $R_2Fe_3Si_5$ (R = Sc, Lu) and (b) $Sc_5Ir_4Si_{10}$. Large green circles are Lu or Sc atoms, medium-sized brown circles are Fe or Ir atoms, and small blue circles are Si atoms.

high-quality single crystals. In the present study, we have grown single crystals of $Lu_2Fe_3Si_5$ and $Sc_2Fe_3Si_5$ and measured the temperature dependence of specific heat down to 0.35 K. All anomalous specific heat features mentioned above are reproduced also in single crystals. In addition, we find a second drop in the specific heat coefficient below 1 K. We can reproduce $C(T)$ reasonably well by assuming two energy gaps. These findings strongly suggest that $Lu_2Fe_3Si_5$ and $Sc_2Fe_3Si_5$ are two-gap superconductors similar to MgB_2 [9]. Band structure calculation and Hall coefficient measurements also support the multiband contributions to the normal state transport properties. We also discuss the anisotropic properties of $R_2Fe_3Si_5$ and the significance of two-gap superconductivity in this system.

$R_5Ir_4Si_{10}$ is also a superconductor where the competition between superconductivity and the charge-density wave is known for all R except for Sc. We have grown high-quality single crystals of $Sc_5Ir_4Si_{10}$ and performed detailed specific heat measurements. $C(T)$ in $Sc_5Ir_4Si_{10}$ is slightly different from that in a weak-coupling superconductor and it is again explained well by assuming two superconducting gaps. However, comparison with $R_2Fe_3Si_5$ suggests that $Sc_5Ir_4Si_{10}$ is a superconductor with an anisotropic energy gap.

2. Experiments

Single crystals of $Lu_2Fe_3Si_5$, $Sc_2Fe_3Si_5$, and $Sc_5Ir_4Si_{10}$ have been grown by the floating-zone technique using an image furnace. The starting rods for the single-crystal growth are prepared by melting a stoichiometric ratio of constituent elements in an arc furnace. We have used lumps of Lu (3Nup), Sc (3Nup), Fe (4N), Ir powder (4N), and Si chips (6N) as starting materials. In the case of $R_2Fe_3Si_5$, as-grown crystals often show lower T_c and broader transitions. In order to improve these characteristics, we have annealed single crystals at ∼1250 °C for an extended period. Lattice parameters for all three single crystals show excellent agreement with published data. Chemical analyses using energy dispersive x-ray spectroscopy reveal that chemical compositions for all three compounds are nearly stoichiometric. Resistivity measurement is performed by the conventional four-probe technique under magnetic fields up to 5 T, and from the results, we estimate the anisotropic upper critical field. The Hall coefficient is measured in the six-probe configuration. Magnetization measurements are performed with a SQUID magnetometer (MPMS-XL5, Quantum Design). Specific heat is measured by the relaxation method with home-built electronics down to 0.35 K using a ^{3}He cryostat.

3. Results and discussion

3.1. $Lu_2Fe_3Si_5$

Figure 2 shows an example of the evolution of resistivity in $Lu_2Fe_3Si_5$ with the duration of annealing at ∼1250 °C. Resistivity decreases and the residual resistivity ratio increases with annealing time. The paramagnetic background magnetization measured at $H = 50$ kOe rapidly decreases at the annealing time of about one week, and it levels off beyond about two weeks, as shown in the inset of figure 2. We speculate that this paramagnetic signal originates either from small impurity phases dispersed in the crystal or the iron defects in the crystal.

Figures 3(a) and (b) show temperature dependences of Hall coefficients for two configurations, $I \parallel c$, $H \parallel ab$ and $I \parallel ab$ $H \parallel c$, respectively [10]. Hall coefficients are negative at room temperature, and their magnitudes are about ten times smaller than those in iron-oxypnictides [11]. However, they show strong temperature dependences, including a sign change for $I \parallel ab$, $H \parallel c$, suggesting contributions from multiple bands, as in iron-oxypnictides. Band structure calculation is carried out by a full potential linearized augmented plane wave (FLAPW) method with the local density approximation for the exchange correlation potential. Resulting Fermi surfaces in $Lu_2Fe_3Si_5$ reveal three bands,

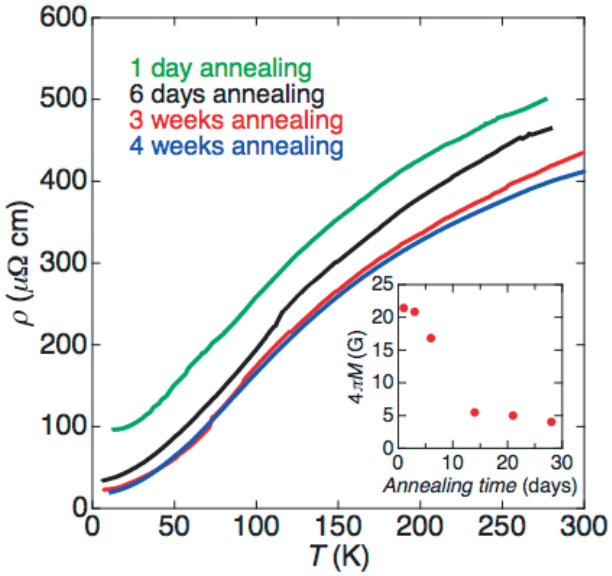

Figure 2. Effect of annealing at 1250 °C on temperature dependence of resistivity in $Lu_2Fe_3Si_5$. Inset shows the magnetization at $H = 50$ kOe for different annealing times.

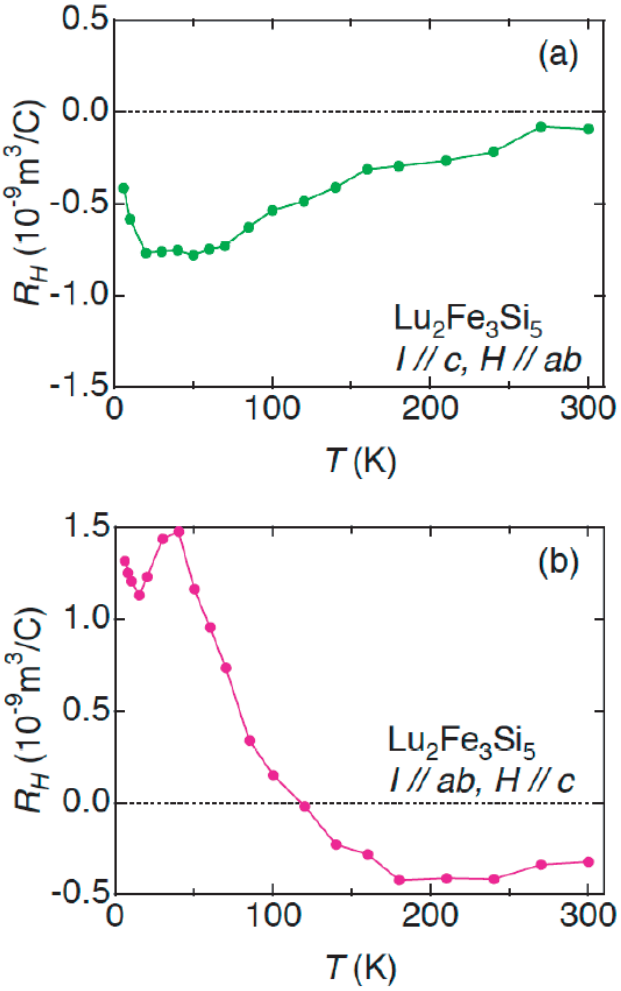

Figure 3. Temperature dependence of Hall coefficient for (a) $I \parallel c$, $H \parallel ab$ and (b) $I \parallel ab$, $H \parallel c$ in $Lu_2Fe_3Si_5$ [10].

as shown in figure 4: two hole bands and one electron band. These results strongly suggest that multiple kinds of carriers are responsible for the normal-state properties in this system.

The temperature dependence of the upper critical field for $Lu_2Fe_3Si_5$ is determined by the midpoint of resistive transition at a constant field. It turns out that $H_{c2}{}^{c}(T)$ is larger than $H_{c2}{}^{ab}(T)$ with an anisotropy parameter of $\gamma \sim 2.0$, indicating that $Lu_2Fe_3Si_5$ is a weakly anisotropic superconductor with one-dimensional anisotropy (not shown) [10, 12]. This value of γ is consistent with the ratio of ρ_c and ρ_{ab} [10, 12], since $\rho_{ab}/\rho_c = (H_{c2}{}^{c}(T)/H_{c2}{}^{ab}(T))^2$. It should be noted that both $H_{c2}(T)$ dependences show extended linear regions in the measured temperature range. Recent measurements of $H_{c2}(T)$ down to 0.4 K confirm this tendency [13].

Figure 5 shows the temperature dependence of specific heat in $Lu_2Fe_3Si_5$. The electronic specific heat jump at T_c, ΔC_e, is strongly reduced from the BCS value of $\Delta C_e/\gamma T_c = 1.43$. At $0.2T_c$, where a BCS superconductor has a small electronic contribution, an appreciable $C_e/\gamma_n T_c$ is observed, which is followed by a second drop below $0.2T_c$. All these anomalies of $C_e/\gamma_n T_c$ are similar to those of MgB_2 with two distinct superconducting gaps originating from the two-dimensional σ-band and three-dimensional π-band [9]. In a two-gap superconductor, electronic specific heat is the sum of two contributions with different gap values, $C_e(T) = x_1 C_1(T) + x_2 C_2(T)$, where $C_1(T)$ and $C_2(T)$ correspond to electronic specific heat from bands 1 and 2, and x_1 and x_2 are the fractional densities of states for bands 1 and 2, respectively. The solid line in figure 5 shows the best fit based on the two-gap model. The two gap values obtained for $Lu_2Fe_3Si_5$ are $2\Delta_1/k_B T_C = 4.4$ and $2\Delta_2/k_B T_C = 1.1$, where $x_1/x_2 = 47/53$ and k_B is the Boltzmann constant. The Arrhenius plot of $C_e(T)$ in the inset of figure 5 shows the slope corresponding to the smaller gap. It should be noted that a similar two-gap analysis has successfully explained the temperature dependence of the penetration depth in $Lu_2Fe_3Si_5$ [14]. However, which of the three bands are responsible for the large or the small gaps is not yet clear.

3.2. $Sc_2Fe_3Si_5$

Figure 6 shows the temperature dependence of resistivity in $Sc_2Fe_3Si_5$. The inset shows a magnification near the transition temperature of ~4.8 K. A small residual resistivity and sharp superconducting transition guarantee the high quality of the measured $Sc_2Fe_3Si_5$ crystal.

Figure 7 shows the temperature dependence of the upper critical field determined by the midpoint of resistive transition for $Sc_2Fe_3Si_5$. Similar to the case of $Lu_2Fe_3Si_5$, $H_{c2}{}^{c}(T)$ is larger than $H_{c2}{}^{ab}(T)$, indicating that $Sc_2Fe_3Si_5$ is also a weakly one-dimensional superconductor. The anisotropy parameter γ is about 2.0, and it is only weakly temperature dependent.

Figure 8 shows the temperature dependence of specific heat in $Sc_2Fe_3Si_5$. The jump in specific heat is again reduced from the BCS value. The solid line in figure 8 shows the

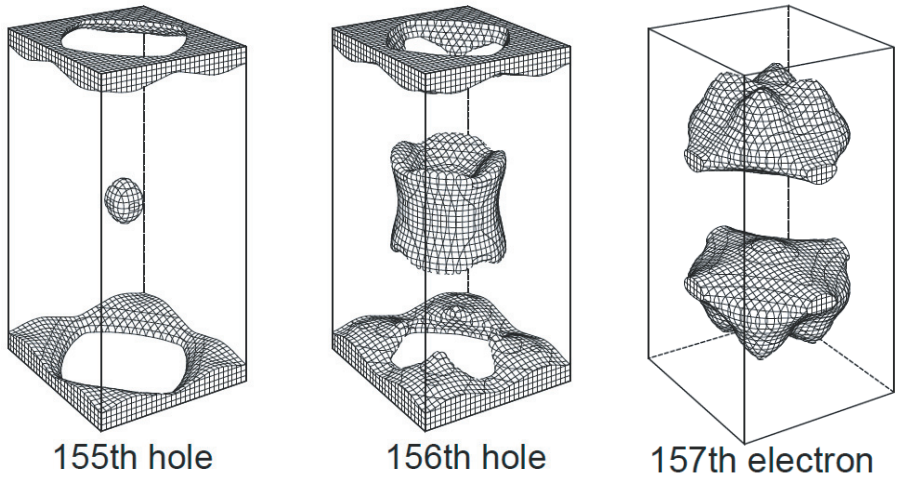

Figure 4. Fermi surfaces of $Lu_2Fe_3Si_5$ calculated by the FLAPW method [10]. Hole-like Fermi surfaces from the (a) 155th and (b) 156th bands, and (c) electron-like Fermi surface from the 157th band are shown.

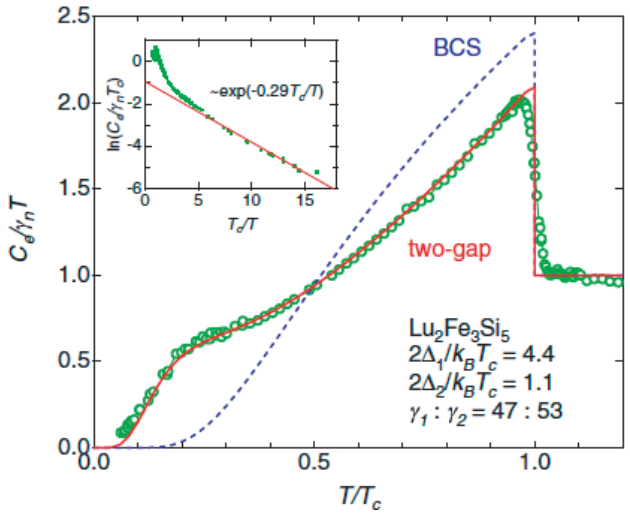

Figure 5. Temperature dependence of specific heat for $Lu_2Fe_3Si_5$ [10]. $C_e(T)$ based on the BCS model is shown by dashed line. The solid line shows the best fit using the two-gap model with $D_1/k_BT_B = 44$ and $D_2/k_BT_B = 1.1$. Inset shows an Arrhenius plot of $C_e(T)$ and suggests the presence of the smaller gap.

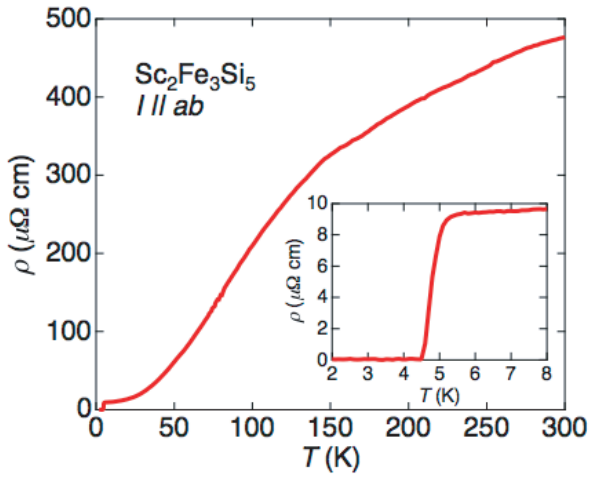

Figure 6. Temperature dependence of resistivity along *ab*-axis for $Sc_2Fe_3Si_5$. Inset shows a magnification close to the superconducting transition temperature.

best fit based on the two-gap model similar to the case of $Lu_2Fe_3Si_5$. The two gap values obtained for $Sc_2Fe_3Si_5$ are $2\Delta_1/k_BT_C = 3.53$ and $2\Delta_2/k_BT_C = 1.7$ with $x_1/x_2 = 36/64$. It is natural to expect a similar two-gap behavior in $Sc_2Fe_3Si_5$ since $Sc_2Fe_3Si_5$ has the same crystal structure as $Lu_2Fe_3Si_5$ with only a slight difference in the lattice parameters.

Here, we stress the uniqueness and importance of two-gap superconductivity in $R_2Fe_3Si_5$. In the case of MgB_2, a well-established two-gap superconductor, the small size of single crystals is an obstacle to many measurements. In $R_2Fe_3Si_5$, however, crystals of millimeter size are readily available. The impurity effect is an important diagnosis to study the gap structure of unconventional superconductors, as in the case of high-temperature superconductors. In $R_2Fe_3Si_5$, we can prepare a complete solid solution of $Lu_2Fe_3Si_5$ and $Sc_2Fe_3Si_5$, where the 3*d* band of iron, responsible for the superconductivity, is intact. In the case of MgB_2, both carbon doping and aluminum doping inevitably introduce charge carriers into the system, in addition to the random potential. This masks the effect of interband scattering. In addition, the orthogonality of σ- and π-bands makes the inter-band scattering probability extremely small, reducing the impurity effects. In $R_2Fe_3Si_5$, no such special situation is anticipated. Hence, this system gives us a unique opportunity to study the effect of interband scattering in two-gap superconductors, which is expected to suppress the larger gap and enhance the smaller gap until they merge. Such a study is now in progress and will be reported elsewhere.

3.3. $Sc_5Ir_4Si_{10}$

Figure 9 shows the temperature dependence of the upper critical field in $Sc_5Ir_4Si_{10}$ with $T_c = 8.4$ K. We define H_{c2} on the basis of the onset of diamagnetism in the magnetization–temperature (M–T) curve or the break in the M–H curve. In $Sc_5Ir_4Si_{10}$, H_{c2} for fields along the *c*-axis, $H_{c2}{}^c$, is larger than for fields in the *ab*-plane $H_{c2}{}^{ab}$ [15].

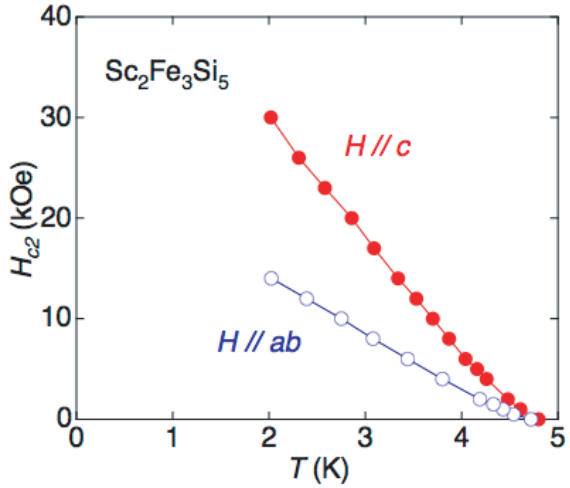

Figure 7. Temperature dependence of upper critical fields, $H_{c2}{}^{c}$ and $H_{c2}{}^{ab}$, estimated from the magnetization-temperature curves for $Sc_2Fe_3Si_5$.

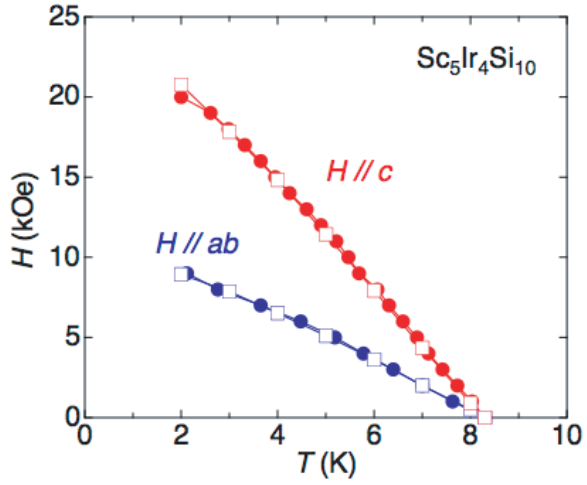

Figure 9. Temperature dependence of the upper critical fields, $H_{c2}{}^{c}$ and $H_{c2}{}^{ab}$, estimated from the M–T (circles) and M–H (squares) curves for $Sc_5Ir_4Si_{10}$.

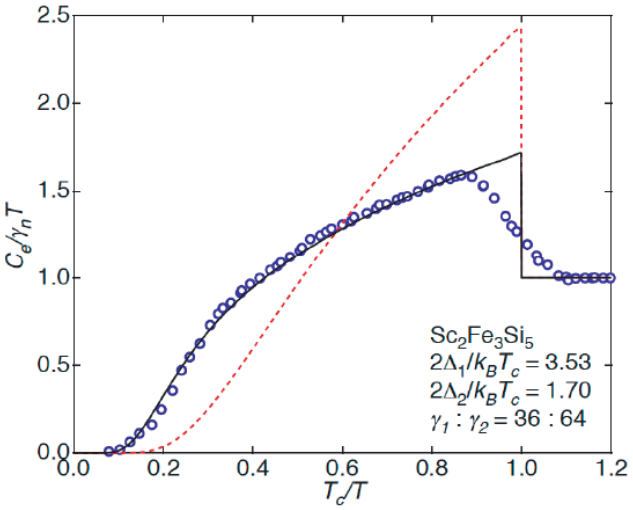

Figure 8. Temperature dependence of specific heat for $Sc_2Fe_3Si_5$. $C_e(T)$ based on the BCS model is shown by dashed line. The solid line shows the best fit using the two-gap model with $D_1/k_BT_B = 3.53$ (36%) and $D_2/k_BT_B = 1.70$ (64%).

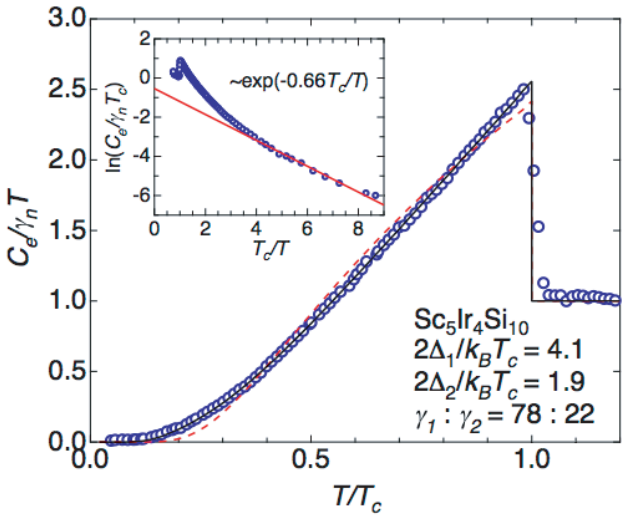

Figure 10. Temperature dependence of specific heat for $Sc_5Ir_4Si_{10}$. $C_e(T)$ based on the BCS model is shown by dashed line. The solid line shows the best fit using the two-gap model. Inset shows Arrhenius plot of $C_e(T)$. The solid line is a guide for the eye suggesting the presence of smaller gap.

The anisotropy parameter γ is again about 2.0, and it is only weakly temperature dependent. This result indicates that $Sc_5Ir_4Si_{10}$ is an anisotropic superconductor with weak one-dimensional anisotropy [15].

Figure 10 shows the temperature dependence of specific heat in $Sc_5Ir_4Si_{10}$. The jump of specific heat at T_c is larger than the BCS value, suggesting that $Sc_5Ir_4Si_{10}$ is a strong-coupling superconductor. The obtained value of the electronic specific heat coefficient γ is 30.5 mJ (mol K^2)$^{-1}$. It should be noted, however, that this value of γ is considerably smaller than the previously reported value of 9.93 mJ (mol K^2)$^{-1}$ for $Sc_5Ir_4Si_{10}$ and is closer to the value of 30.9 mJ (mol K^2)$^{-1}$ for $Sc_5Co_4Si_{10}$ [16]. Actually, recent nuclear magnetic resonance studies on $Sc_5Co_4Si_{10}$, $Sc_5Ir_4Si_{10}$, and $Sc_5Rh_4Si_{10}$ show rather similar values of the density of states at the Fermi level in these three compounds [17]. Therefore, we believe that our value of γ is more intrinsic. Coming back to figure 10, the broken line shows the BCS temperature dependence of the electronic specific heat coefficient with $2\Delta/k_BT_c = 3.53$. A systematic deviation is obvious. The BCS formula with different values of $2\Delta/k_BT_c$ also does not fit the data. Such a discrepancy between the experimental result and the theory can be amended by assuming two superconducting gaps. The solid line in figure 10 shows the best fit based on the two-gap model similar to the case of $Lu_2Fe_3Si_5$. The two gap values obtained for $Sc_5Ir_4Si_{10}$ are $2\Delta_1/k_BT_c = 4.1$ and $2\Delta_2/k_BT_c = 1.9$ with $x_1/x_2 = 78/22$. The Arrhenius plot of $C_e(T)$ in the inset of figure 10 shows the slope corresponding to the smaller gap.

Here, we discuss the plausibility of the two-gap scenario in $Sc_5Ir_4Si_{10}$. Strictly speaking, $C_e(T)$ in most superconductors deviates from the simple weak-coupling BCS formula. Recently, the two-gap feature was also reported in Nb_3Sn [18]. Huang *et al* analyzed $C_e(T)$ in YNi_2B_2C with different gap symmetries including the two-gap model [19].

They concluded that both the point-node model and the two-gap model fit the experimental data equally well. In the case of $Lu_2Fe_3Si_5$, and possibly also $Sc_2Fe_3Si_5$, two-gap analyses have a rather firm ground since we do observe a clear second drop in $C_e(T)$ at lower temperatures. In other words, the smaller gap has a markedly different gap value from the larger one with significant fraction. In the case of $Sc_5Ir_4Si_{10}$, the deviation of $C_e(T)$ from the BCS model is too small, and correct gap structure can be identified only by combining other experimental results such as impurity effects. In this sense, T_c being almost independent of the Lu content in $(Lu_{1-x}Sc_x)_5Ir_4Si_{10}$ [20] might suggest that $Sc_5Ir_4Si_{10}$ is a superconductor with a weak gap anisotropy rather than a two-gap superconductor.

4. Summary

The temperature dependence of specific heat in the silicide superconductors $Lu_2Fe_3Si_5$, $Sc_2Fe_3Si_5$, and $Sc_5Ir_4Si_{10}$ were investigated down to 0.35 K. The phenomenological two-gap model reproduced $C_e(T)$ reasonably well in all compounds. Although the two-gap scenario for superconductivity has a firm ground for $Lu_2Fe_3Si_5$ and $Sc_2Fe_3Si_5$, a superconductor with a weak gap anisotropy might be more appropriate for $Sc_5Ir_4Si_{10}$. It was also found that all these compounds are anisotropic superconductors with weak one-dimensional anisotropy.

Acknowledgment

This work is supported by a Grant-in-Aid for Scientific Research from the Ministry of Education, Culture, Sports, Science, and Technology.

References

[1] Braun H F 1980 *Phys. Lett.* A **75** 386
[2] Braun H F and Segre C U 1980 *Solid State Commun.* **35** 735
[3] Steglich F, Aarts J, Bredl C D, Lieke W, Meschede D, Franz W and Schafer H 1979 *Phys. Rev. Lett.* **43** 1892
[4] Shirotani I, Kihou K, Sekine C, Takeda N, Ishikawa M and Yagi T 2003 *J. Phys.: Condens. Matter* **15** S2201
[5] Kamihara Y, Watanabe T, Hirano M and Hosono H 2008 *J. Am. Chem. Soc.* **130** 3296
[6] Ren Z A *et al* 2008 *Chin. Phys. Lett.* **25** 2215
[7] Vining C B, Shelton R N, Braun H F and Pelizzone M 1983 *Phys. Rev.* B **27** 2800
[8] Tamegai T, Nakagawa T and Tokunaga M 2007 *Physica* C **460–462** 708
[9] Bouquet F, Fisher R A, Phillips N E, Hinks D G and Jorgensen J D 2001 *Phys. Rev. Lett.* **87** 047001
[10] Nakajima Y, Nishizaki T, Tamegai T and Harima H 2008 *Phys. Rev. Lett.* **100** 157001
[11] Chen G F *et al* 2008 *Phys. Rev. Lett.* **101** 057007
[12] Tamegai T, Nakajima Takagawa T, Li G J and Harima H *J. Phys.: Conf. Ser.* at press
[13] Nakajima Y, Nishizaki T, Sasaki T, Kobayashi N and Tamegai T, unpublished
[14] Gordon R, Vannette M D, Martin C, Nakajima Y, Tamegai T and Prozorov R 2008 *Phys. Rev.* B **78** 024514
[15] Li G J, Miura M, Shi Z X and Tamegai T 2007 *Physica* C **463–465** 76
[16] Hausermann-Berg L S and Shelton R N 1987 *Phys. Rev.* B **35** 6659
[17] Lue C S, Liu R F, Fu Y F, Cheng C and Yang H D 2008 *Phys. Rev.* B **77** 115130
[18] Guritanu V, Goldacker W, Bouquet F, Wang Y, Lortz R, Goll G and Junod A 2004 *Phys. Rev.* B **70** 184526
[19] Huang C L, Lin J-Y, Sun C P, Lee T K, Kim J D, Choi E M, Lee S I and Yang H D 2006 *Phys. Rev.* B **73** 012502
[20] Yang H D, Klavins P and Shelton R N 1991 *Phys. Rev.* B **43** 7681